

CLEARING RESIDUAL PLANETESIMALS BY SWEEPING SECULAR RESONANCES IN TRANSITIONAL DISKS: A LONE-PLANET SCENARIO FOR THE WIDE GAPS IN DEBRIS DISKS AROUND VEGA AND FOMALHAUT

XIAOCHEN ZHENG (郑晓晨),¹ DOUGLAS N. C. LIN (林潮),^{2,3,4} M. B. N. KOUWENHOVEN (柯文采),⁵
SHUDE MAO (毛淑德),^{1,4,6} AND XIAOJIA ZHANG (张晓佳)⁴

¹*Department of Physics and Center for Astrophysics, Tsinghua University, Beijing 10086, P.R. China*

²*Institute for Advanced Studies, Tsinghua University, Beijing 10086, P.R. China*

³*Department of Astronomy and Astrophysics, University of California, Santa Cruz, CA 95064, USA*

⁴*National Astronomical Observatories of China, Chinese Academy of Sciences, 20A Datun Road, Beijing 100012, P.R. China*

⁵*Department of Mathematical Sciences, Xi'an Jiaotong-Liverpool University, 111 Ren'ai Rd., Suzhou Dushu Lake Science and Education Innovation District, Suzhou Industrial Park, Suzhou 215123, P.R. China*

⁶*Jodrell Bank Centre for Astrophysics, School of Physics and Astronomy, The University of Manchester, Oxford Road, Manchester M13 9PL, UK*

ABSTRACT

Extended gaps in the debris disks of both Vega and Fomalhaut have been observed. These structures have been attributed to tidal perturbations by multiple super-Jupiter gas giant planets. Within the current observational limits, however, no such massive planets have been detected. Here we propose a less stringent ‘lone-planet’ scenario to account for the observed structure with a single eccentric gas giant and suggest that clearing of these wide gaps is induced by its sweeping secular resonance. With a series of numerical simulations, we show that the gravitational potential of the natal disk induces the planet to precess. At the locations where its precession frequency matches the precession frequency the planet imposes on the residual planetesimals, their eccentricity is excited by its resonant perturbation. Due to the hydrodynamic drag by the residual disk gas, the planetesimals undergo orbital decay as their excited eccentricities are effectively damped. During the depletion of the disk gas, the planet’s secular resonance propagates inward and clears a wide gap over an extended region of the disk. Although some residual intermediate-size planetesimals may remain in the gap, their surface density is too low to either produce super-Earths or lead to sufficiently frequent disruptive collisions to generate any observable dusty signatures. The main advantage of this lone-planet sweeping-secular-resonance model over the previous multiple gas giant tidal truncation scenario is the relaxed requirement on the number of gas giants. The observationally inferred upper mass limit can also be satisfied provided the hypothetical planet has a significant eccentricity. A significant fraction of solar or more massive stars bear gas giant planets with significant eccentricities. If these planets acquired their present-day kinematic properties prior to the depletion of their natal disks, their sweeping secular resonance would effectively impede the retention of neighboring planets and planetesimals over a wide range of orbital semi-major axes.

Keywords: planetary systems – stars: individual (Vega, Fomalhaut) – methods: numerical – planet-disk interaction– protoplanetary disks

1. INTRODUCTION

Debris disks are common around nearby young stars (Morales et al. 2013). Infrared and sub-millimeter observations have revealed that some of these disks have wide (> 10 AU) gaps separating a compact (a few AU in size) inner disk from an extended outer ring. For example, the observed excess emission for wavelengths $\lambda \geq 15 \mu\text{m}$ in the debris disk around ϵ Eri indicates the presence of a gap between two narrow rings (Backman et al. 2009). The debris disk around HR8799 contains an inner warm belt, a broad cold belt and an outer halo (Su et al. 2009). Two additional debris systems with widely separated inner disks and outer rings were found around Vega and Fomalhaut (Su et al. 2013). Just like HR8799, the central stars of these disks are all more massive than the Sun. More recently, Morales et al. (2013) announced the discovery of four additional debris disks with widely separated belts around HD70313, HD71722, HD159492 and HD104860.

These two-component debris disks show some resemblance to the kinematic architecture of our own Solar system, which contains the inner asteroid belt and the outer Kuiper belt. Between these two belts, gravitational perturbation of the two gas giants and two ice giants may have destabilized the orbits and cleared residual planetesimals in the region both during their formation epoch and during the subsequent dynamical evolution of the Solar System (Duncan et al. 1989). In particular, after the solar nebula was removed, large amount of material was swept inward producing a high radial mass concentration in the inner region of the Solar system, finally leading to the formation of terrestrial planets and leaving small amount of debris known as the asteroid belt we observe today (Thommes et al. 2008; Zheng et al. 2017; Bromley & Kenyon 2017). The dynamical sculpting process of the multiple giant planets on the formation of the present-day's Kuiper Belt, may

have proceeded over several 10^8 yrs (Levison et al. 2008).

This similarity suggests that it may be possible to infer the presence of one or more exoplanets from the surface brightness distribution of disks around other stars. Indeed, Kalas et al. (2008) reported a possible faint planetary companion around Fomalhaut. It has been attributed as a potential culprit for dynamically shaping the ring-like outer debris disk around Fomalhaut (Chiang et al. 2009). But, this interpretation on the physical nature of this candidate remains controversial (Janson et al. 2012; Boley et al. 2012). Regardless its validity, its mass is too low to account for the wide gap between the inner and outer regions of Fomalhaut's disk.

In order for single gas giants to open a wide gap in the debris disks around Vega and Fomalhaut, their masses must exceed several tens of Jupiter masses. Such conspicuous massive companions have not been found (Marois et al. 2006; Heinze et al. 2008; Su et al. 2013). Partial clearing of planetesimals and grains over an extended region may also be induced by single less massive (still many times that of Jupiter) planets on highly eccentric ($e > 0.8$) orbits. The excitation, stability, and retention of such massive, highly eccentric, single planets with such large eccentricities and semi-major axis remain an outstanding issue.

Su et al. (2013) attributed the combined tidal perturbation of one or multiple planets as the culprit for the large dust-free gap in the debris disks. Each planet has a chaotic zone within which the orbits of other planets and planetesimals are destabilized by long-term dynamical instabilities. Similar to the Solar System, four or more Jupiter-mass planets are needed to fill the wide gap with their overlapping chaotic zones. But, the analysis of the combined data from direct imaging, microlensing, and radial velocity survey shows a precipitous decline in the

abundance of planets with masses larger than Neptune in all period ranges (Clanton & Gaudi 2016), although there are a few known gas giants beyond ~ 100 AU from the host stars. In contrast, Neptune-mass/size planets are common at a distance of less than 1AU from their host stars. A slightly sparser population of distant Neptune-mass planets has been extrapolated from the statistical properties of their close-in cousins. This inference has not been observationally verified because these planets have masses which are below the detection threshold. Since the width of the chaotic zone around any host stars increases with their masses, additional Neptune-mass planets (in comparison with Jupiter-mass planets) are needed to provide an adequate filling factor of their chaotic zones over the wide gap regions.

The key challenge for clearing wide gaps by embedded planets is their limited zone of influence. Due to secular interactions, eccentric planets can perturb other planets and residual planetesimals beyond the chaotic zone. These perturbations are generally weak. However, gravitational interactions with the natal disks also leads to the precession of embedded planets. The planets' mutual secular perturbations also induce nodal precession and eccentricity modulation. In resonant locations where the disk-induced precession rate matches to that due to planets' interaction with each other, persistence of the relative longitude of periapses of the interacting planets can lead to large eccentricities.

Through secular interactions, multiple planets undergo eccentricity modulations and apsidal precession with distinct eigen frequencies (Murray & Dermott 1999). In the solar system, Jupiter and Saturn also impose secular perturbations to asteroids in the main belt. In some special locations, asteroids precess at rates close to gas giants' apsidal precession rate. These asteroids attain longitudes of periapse at a nearly

constant (non-zero) phase relative to that of Jupiter such that their eccentricities are largely excited. Although these zones of (ν_5 and ν_6) secular resonances are narrowly confined, they can extend well outside the chaotic zones. Furthermore, the location of the secular resonances can evolve with the eigen-frequencies of the system. The Nice model is constructed based on the assumption that, due to a hypothetical widening of Jupiter-Saturn separation, the ν_5 secular resonance may have propagated between the main belt region and its current location (interior to the orbit of Venus). Gomes et al. (2005) proposed that, along the propagation paths of the ν_5 secular resonance, the eccentricities of some asteroids were greatly excited so that they were cleared out of the main belt region and became the culprits of the Lunar "late heavy bombardment". This hypothesis remains controversial because it is also likely to excite the eccentricities of the terrestrial planets to values much higher than the present-day observed values (Brasser et al. 2009; Agnor & Lin 2012).

There are other effects which can lead to the efficient clearing of planetesimals and planets. Gas giant planets were formed in gas-rich protostellar disks. With sufficient masses, the tidal perturbation of these embedded gas giants induce the formation of a gap in the disk's gas distribution (Bryden et al. 2000). Hydrodynamic simulations show that this process also leads to dust clearing and filtration. In the case of single-planet systems, the width of the gap is typically a few Hill radii, and less than the distance between the planet and its 2:1 mean motion resonance (Zhu et al. 2011, 2012). With this limited perturbation on the gas and dust distribution, many hypothetical gas giants would be needed to clear the wide gaps in the disks around Vega and Fomalhaut.

The gravity of the planets' natal disks can also lead to the precession of their orbits. In a minimum mass nebula this effect dominates the

secular perturbation between planets. As the disks' contribution to the total gravity reduces during the depletion, the planets' precession rate due to the disk potential declines. Consequently, the location of their secular resonance propagates over wide regions. In the Solar System, the ν_5 and ν_6 secular resonances sweep across the inner regions of the solar nebula (where the terrestrial planets are located). This effect leads to the excitation of residual planetesimals' eccentricities by the major planets, even at those large distances (Heppenheimer 1980; Ward 1981; Nagasawa et al. 2003).

The diminishing residual disk gas also damps the eccentricity of the planetesimals, which leads to the decay of their orbits (Nagasawa et al. 2003, 2005). Since the ν_5 and ν_6 secular resonances interior to the gas giants' orbits also propagate inwards, the residual planetesimals caught along their paths continue to migrate inward. This process may have led to (i) a significant clearing of the asteroid belt (Zheng et al. 2017); (ii) a high concentration and dynamical shake-up of planetesimals interior to the orbit of Mars (Zheng et al. 2017); and (iii) it may have promoted the formation and subsequent eccentricity damping of the terrestrial planets (Thommes et al. 2008). This model is consistent with the formation time scale of the terrestrial planets ($\sim 10^{7-8}$ yr) inferred from radioactive isotopes and the small orbital eccentricities ($e < 0.1$) of the terrestrial planets.

Here, we propose that the observed wide gaps in some debris disks may have been cleared by the secular resonances of a known planetary candidate (in Fomalhaut) or yet to be detected (around Vega and other systems) isolated or multiple gas giants or super Neptunes, as the secular resonances sweep across this region during the depletion of the gas disk. Analogous to the asteroids, excited eccentricities of the residual planetesimals in the region between the inner disk and outer ring are mainly damped by

the hydrodynamic drag of the diminishing disk gas. In addition to the extended gap, this scenario offers a potentially exciting prospect of finding signatures of ongoing planetary assemblage in debris disks around stars with an age comparable to the formation epoch of terrestrial planets in the solar system (Su et al. 2009).

Since not a single planet with a mass in excess of $\sim 1M_J$ (an observationally inferred upper limit) has been found around Vega and Fomalhaut, we explore here the possibility that the extensive gaps are produced by a sweeping secular resonance of a lone-planet with a modest mass and eccentricity in the debris disks around these and other similar systems. Although systems of multiple Neptune-mass planets may also lead to a similar effect, we opt the lone-planet scenario as an idealized simplest possibility.

This paper is organized as follows: in §2, we briefly introduce the lone-planet possibility in the Vega system, including detailed physical models to mimic the dust-free gap opening process by lone-planet scenario in Vega system, develop a rough method to constrain planet candidates based on observed features, and provide predictions for future planet detection. In §3, we further extend our model to Vega-like system, Fomalhaut, inferring the properties of the prospective planet and compare these with a planet candidate, Fomalhaut b. A summary of our results and an extensive discussion on the other two belt debris disks are presented in §4.

2. A LONE-PLANET SCENARIO FOR THE VEGA SYSTEM

2.1. *Dynamical causes for wide dust-free gaps in debris disks*

Infrared observations indicate that Vega's debris disk contains a large gap that spans from ~ 15 AU to ~ 110 AU (Su et al. 2013). The relatively large size of the gap in Vega's debris disk can be used to constrain the orbital configuration of Vega's (hypothetical) planetary sys-

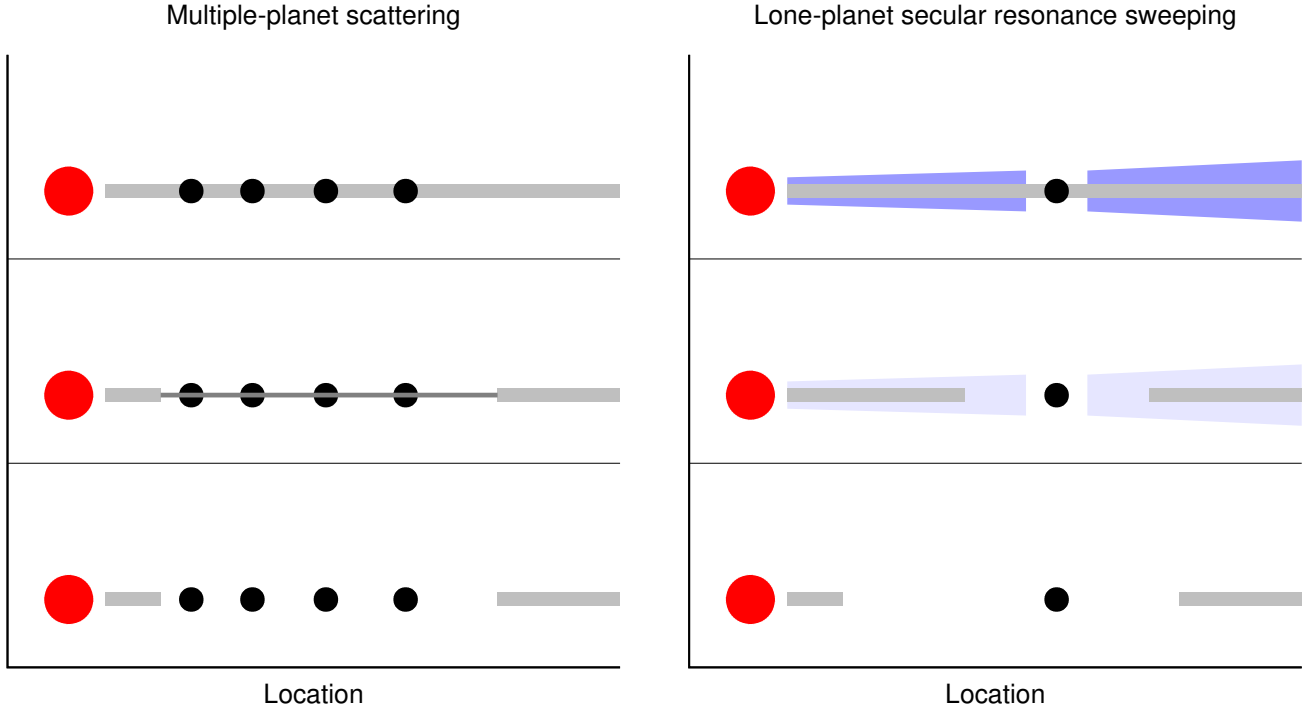


Figure 1. A schematic representation comparing the multiple-planet scenario (left) with the lone-planet scenario (right). The red solid dots refer to the host star, while gray bars and blue-shaded areas label the possible distribution of planetesimal disk and a depleting gas disk, respectively. From top to bottom, two models both describe the orbital evolution of a planetary system from an early age to the present day. The thinning (or shrinking) of the gray bars on planetesimal disk as well as the fading blue areas of the gas disk indicate their decreasing surface density.

tem. In our solar system, the four gas giants cleared most of the debris between the outer asteroid belt ~ 3 AU and the inner Kuiper belt ~ 35 AU. Similarly, in the young HR 8799 system, (at least) four giant planets have been detected (Marois et al. 2008, 2010) and they are believed to be the chief culprit for the large separation between the warm ($\sim 6 - 15$ AU) and cold ($\sim 90 - 300$ AU) debris disks (Su et al. 2009). Therefore, a multiple-planet configuration is a preferred scenario in the Vega and Vega-like systems which has a characteristic debris disk with two broadly separated compo-

nents. Su et al. (2013) claims that the deficit of planetesimals orbiting Vega with semi-major axes in the range $15 - 110$ AU can be attributed to the existence of multiple, currently undetected planets. However, in our study we discuss the possibility of a single planet with an intermediate mass (few M_J) and intermediate orbital eccentricity that can produce this gap.

Motivated by earlier works on the dynamic shake-up model (Nagasawa et al. 2005; Thommes et al. 2008), we focus on the dynamical evolution of a debris disk around the star, in the presence of a single gas giant and a depleting

circumstellar gas disk. The evolution of the debris disk (planetesimal disk) is affected by the gravitational potential of both the gas giant and the gas disk, and also by the hydrodynamical drag due to the protoplanetary gas disk. Generally, secular resonances occur when the precession rate of the gas giant caused by the gas disk potential matches that of planetesimals in the debris disk, whose precessions are modulated by both the gas disk and the gas giant. After being captured into secular resonance, the planetesimals are excited and generally migrate away from their original orbits due to subsequent damping. As the gas disk depletes over time, the location of the secular resonance also sweeps inward, through the debris disk. This provides a possible explanation for the large dust-free gap structures in the debris disks of Vega-like systems. In order to clear the gap region, it is therefore necessary for the secular resonance to sweep through the entire region where the dust infrared emission is observed to be absent.

Even though the evolution process especially the planetesimal clearing mechanisms of these two scenarios are quite different, theoretically, both models can reproduce the present-day debris disk observation (see Figure 1).

2.2. Model Setup

2.2.1. The Circumstellar Gas Disk

As we aim at the dynamical evolution of a swarm of planetesimals which are embedded in a depleting gas nebula, we modified the publicly available HERMIT4 package (Aarseth 2003) by adding an analytical disk potential and hydrodynamic drag on particles, as described in Zheng et al. (2017) for details. Briefly, a radial surface density distribution for the gas disk of the form

$$\Sigma(r, t) = \Sigma_0 \exp(-t/T_{\text{dep}}) r^{-k}, \quad (1)$$

is adopted, where Σ_0 is the fiducial surface density of gas disk at 1 AU, and T_{dep} is the depletion

time scale of the gas disk. In the *minimum mass nebula model* (Hayashi et al. 1985), $\Sigma_0 = 1,000 - 2,000 \text{ g cm}^{-2}$ and a power law index $k = 1.5$ are widely used for describing our solar system and solar-like systems at early times (e.g., Nagasawa et al. 2005). The best estimate for Vega’s age is around 450 Myr (Yoon et al. 2010). A representative depletion timescale, $T_{\text{dep}} = 1 - 5 \text{ Myr}$, is mainly discussed in this paper.

The presence of a (< few) Jupiter-mass planet not only perturbs nearby planetesimal disk, but its tidal interaction with gas also affects the morphology of the disk by opening a gap in the surface density distribution (Lin & Papaloizou 1986). The gap structures (the depth and width of the gap) are closely related to the planet’s eccentricity and mass, especially for a planet with an eccentricity above its Hill radius, $r_{\text{Hill}} \sim a_p (\frac{m_p}{M})^{\frac{1}{3}}$, divided by its semi-major axis a_p (Hosseinbor et al. 2007). For computational simplicity, we conservatively estimate a gas-free gap in the region around $a_p \pm r_{\text{Hill}}$.

2.2.2. The Planetesimal Disk

In our model, a planetesimal disk (debris disk) coplanar to the assumed planet and overlaps with the gas disk. We assume that all planetesimals and gas particles within the Hill radii region of the hypothetical planet are totally accreted (or depleted), the motion of planetesimals is determined by the central star and the disk’s gravity beyond the gap region. Since most planetesimals are located outside the gap region, they are subject to the disk’s self gravity from nearby regions (Nagasawa et al. 2005; Zheng et al. 2017). The eccentricity of planetesimals is also damped by their tidal interaction with the residual disk gas. When the total damping timescale, T_{damp} , is shorter than or comparable to the gas depletion timescale, T_{dep} , of the protostellar disk, the planetesimals migrate inwards with the secular resonances’ inwardly sweeping rate. This combined influ-

ence of the planet’s secular perturbation and the disk gas’ eccentricity damping clear planetesimals over large region of the disk.

Throughout this work, we consider km-size planetesimals. These particles are the most likely parent bodies of μm and mm-size collisional fragments which are mostly to be responsible for the observed inferred features of the Vega and Vega-like system (Wyatt & Dent 2002). In this size range, eccentricity damping of planetesimals is mainly caused by the hydrodynamic drag, which is inversely proportional to the planetesimal radius. Therefore, if the hypothetical planet can efficiently clear the \sim km planetesimals, it would also be effective in opening up a wide gap for the sub-km size planetesimals.

2.3. Boundary Constraints

Under the assumption that there is indeed a single, undetected giant planet in the debris disk, the observed disk boundaries provide constraints on its orbital parameters (in particular, its mass m_p , semi-major axis a_p and eccentricity e_p). In general, the presence of a gas giant planet can generate a chaotic zone surrounding its orbit. Within this zone, it is essentially impossible for planetesimals to attain stable orbits. The dynamical origin for this chaotic zone is mainly due to the overlap of mean motion resonances (Wisdom 1980). The width of the chaotic zone is related to the planet-to-star mass ratio, μ . According to Morrison & Malhotra (2015), particles in a planet’s chaotic zone are mostly (95%) driven out. For an eccentric planet with $e_p > 0.2$ and $10^{-9} \leq \mu \leq 10^{-1.5}$, the interior and exterior boundaries for the chaotic zone are not asymmetric about the planet’s orbit and they are located at separations

$$\delta a_{\text{int}} \approx 1.2 \mu^{0.28} r_p, \quad (2)$$

and

$$\delta a_{\text{ext}} \approx 1.7 \mu^{0.31} r_a, \quad (3)$$

respectively, where $r_p = a_p(1 - e_p)$ and $r_a = a_p(1 + e_p)$ are its periastron and apoastron distance from its host star. Su et al. (2015) have suggested that the wide gap between the outer boundary of the warm and inner boundary of the cold debris belt around HD 95086 may due to the clearing of planetesimals in the chaotic zones of multiple hypothetical planets in addition to the confirmed exoplanet (Rameau et al. 2013, 2016). Similar scenario of dynamical clearing by multiple, massive, undetected planets have been invoked to account for the wide, dust-free gaps in several other systems including the ϵ Eridani system (Su et al. 2017) and the HIP 67497 system (Bonnefoy et al. 2017).

In the lone-planet scenario, we suggest that residual planetesimals may be cleared well beyond the region between a_{int} and a_{ext} during the epoch of disk depletion. The disk’s gravitational potential leads to precession of any embedded planet’s orbit. As this contribution to the gravity weakens with the decline in the disk’s surface density, the planet’s precession slows down and the location of its secular resonance expands from the proximity of its orbit to far-flung regions in the disk. During the passage of the secular resonance, the planetesimals’ eccentricity is excited as their angular momentum is removed by the planet’s tidal torque. Subsequent damping of the planetesimals’ eccentricities by the hydrodynamic drag of the residual disk gas dissipates their orbital energy and induces them to undergo orbital decay.

In the region interior to the planet’s orbit, the inwardly migrating planetesimals endure a prolonged resonant perturbation as their orbital evolution proceeds in the same direction as the propagation of the planet’s inner secular resonances. Despite the gas depletion, an efficient damping rate of planetesimals’ eccentricity is maintained as they enter into the dense inner regions where $T_{\text{damp}}/T_{\text{dep}} < 10$ (for example, see Figure 2). Consequently, residual planetes-

imals interior to the planet’s orbit can migrate over extensive distances and the inner boundary of the dust-free gap is strongly affected by the sweeping secular resonance mechanism.

In the region outside the planet’s orbit, the outward propagation of its secular resonance diverges from the orbital decay of the planetesimals along its path. During the single passage of the secular resonance, the amplitude of eccentricity excitation of the perturbed planetesimals is relatively modest (see also Figure 2). As the secular resonance expands to large radii, the local eccentricity damping rate of the perturbed planetesimals also diminishes with the decrease in the surface density of the disk gas such that $T_{\text{damp}}/T_{\text{dep}} \gg 1$ (see Eq. 1). The weakened contribution of the sweeping secular resonances implies that the outer boundary of the cleared region may be mainly determined by the stability condition in Equation (3), although some planetesimals may diffuse into the chaotic zone shortly after the passage of the secular resonance.

These considerations indicate that after the gas in a disk with an embedded distant giant planet is severely depleted, a wide gap is expected to form between an inner warm and an outer cold belt. The outer edge of the warm belt is mostly sculpted by the planet’s sweeping secular resonance whereas the inner cavity of the cold belt essentially extends throughout the planet’s exterior chaotic zone. Based on this conjecture, we use the observed gap structure in the Vega system to place several quantitative constraints on the embedded planet’s mass m_p , semi-major axis a_p and eccentricity e_p (Fig. 3).

We first satisfy the constraints set by the outer boundary of the detected dust-free gap (the inner boundary of the cold belt) $r_{\text{out}} = 110$ AU under the assumption $r_{\text{out}} \simeq a_{\text{ext}}$. From Equation 3, we find an $a_p - e_p$ relation for each of three representative planet masses: M_S (Saturn mass), M_J (Jupiter mass), and $3M_J$ which is an

observational upper mass limit for any hypothetical planet in the region between ~ 20 AU and ~ 70 AU around Vega (Marois et al. 2006; Heinze et al. 2008).

For each set of planetary orbital parameters, we find effects of the planet’s secular resonance on the residual planetesimals interior to the planet’s orbit. In general, the location and clearing efficiency of the secular resonance are determined by $\Sigma(r, t)$, m_p , a_p , and e_p (Nagasawa et al. 2003, 2005; Thommes et al. 2008). With a generic prescription for $\Sigma(r, t)$ (Eq. 1) we compute the dynamical evolution of planetesimals’ orbits as the disk becomes severely depleted at $t = 10T_{\text{dep}}$. Two sets of T_{dep} (1 and 5 Myr) are used to evaluate whether the outcome may depend on its magnitude. In all cases, the inner secular resonance has propagated well inside 10 AU with a local $T_{\text{damp}} < T_{\text{dep}}$ while the outer secular resonance has propagated well outside 150 AU with a local $T_{\text{damp}} > 10^3 T_{\text{dep}}$ at this epoch.

In order to examine whether the sweeping secular resonance can actually clear a region down to the observed inner boundary of the gap $r_{\text{in}} = 15$ AU, we consider a population of test planetesimals with an initial circular orbit at 15 AU from the host star. There are three potential outcomes for the perturbed planetesimals: (i) those that are excited by secular resonance and experience efficient damping, resulting in an inward migration; (ii) those that are insignificantly perturbed by the secular resonance and remain in the proximity of their original locations; and (iii) those that are highly excited by secular resonance but the gas drag is ineffective to damp their eccentricity, resulting in escape from the system.

For the purpose of placing constraints on the hypothetical planet’s orbital properties with the observed structure of Vega’s debris disk, we neglect category (iii) and distinguish the retained planetesimals in categories (i) and (ii) by their

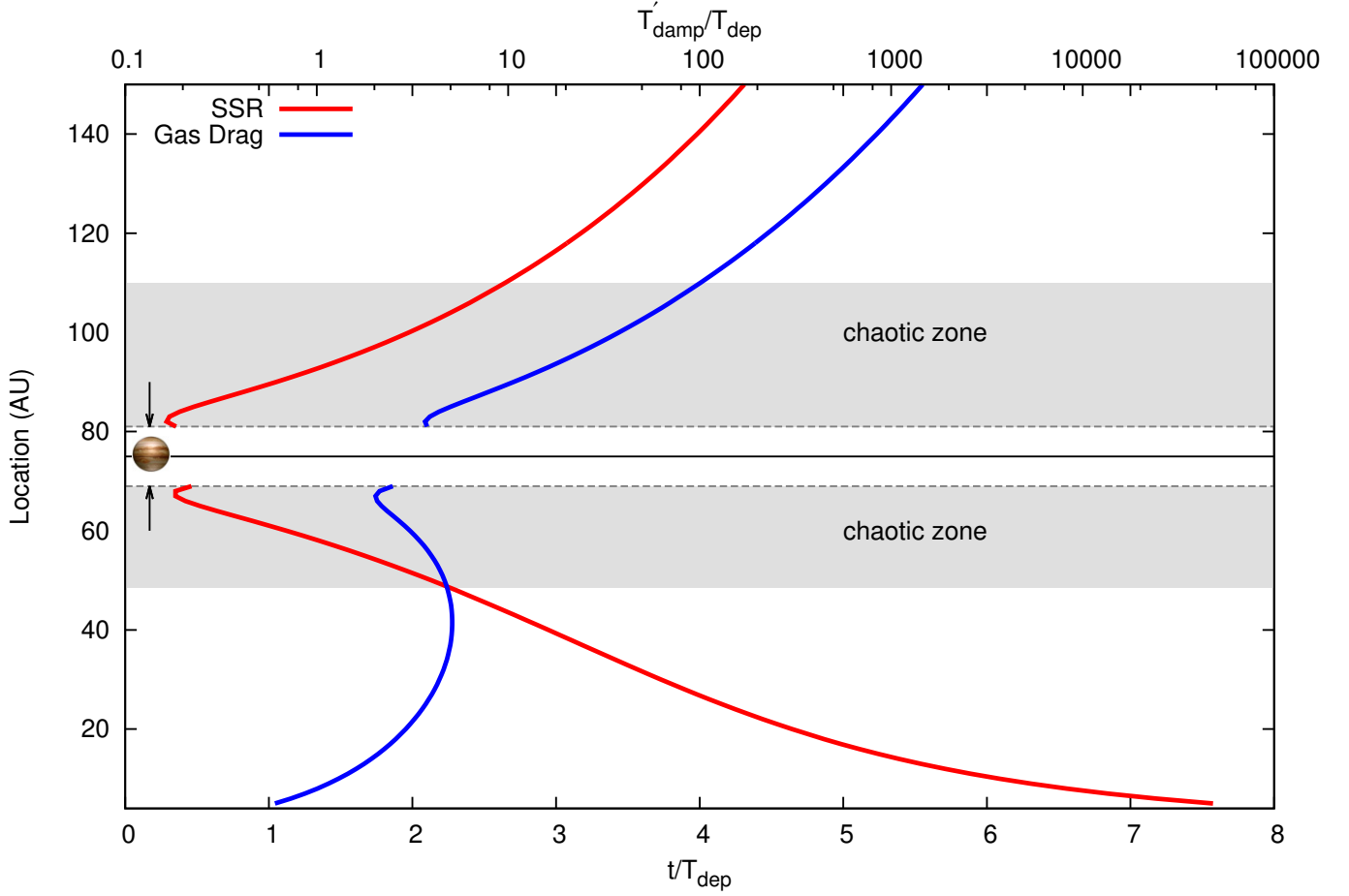


Figure 2. Location of a hypothetical planet’s inner and outer secular resonances (red curve) as a function of the depletion factor t/T_{dep} . The depletion timescale $T_{\text{dep}} = 5$ Myr, the planet’s $m_p = 3M_J$, $a_p = 75$ AU, and $e_p = 0.2$ so that its $a_{\text{int}} \sim 50$ AU and $a_{\text{ext}} \sim 110$ AU. The location of secular resonances have propagated beyond a_{int} and a_{ext} at $t/T_{\text{dep}} \simeq 3$. At the location of the secular resonance, the eccentricity damping efficiency is inversely proportional to the magnitude of $T'_{\text{damp}}/T_{\text{dep}}$ (blue curve). The solid line represent the orbital semi major axis of the planet and the dotted black lines indicate the width of a gas-free zone.

final semi-major axis at $t = 10T_{\text{dep}}$ (indicated by the color bar in Figure 3). These results indicate that the sweeping secular resonance of a lone planet with modest mass can effectively excite planetesimals’ eccentricity and induce significant orbital decay provided it has adequate eccentricity. For each planet with a mass m_p , there is a set of critical a_p and e_p (marked by light blue filled circles in Figure 3) which delineates categories (i) and (ii). The critical values of a_p (in Fig. 3) is $\sim 63 - 67$ AU for all three different m_p with $T_{\text{dep}} = 1$ Myr whereas

those of e_p decreases from 0.57 for $m_p = M_S$ to 0.33 for $m_p = 3M_J$. With a longer $T_{\text{dep}} (= 5$ Myr), the critical values of $a_p \simeq 68 - 75$ AU and $e_p \simeq 0.45 - 0.2$ for $m_p = M_S - 3M_J$.

2.4. Single Planet Architecture

In the previous section, we placed several constraints on the hypothetical planet’s orbital parameters with a single planetesimal which was initially placed at 15 AU. In this section, we consider the evolution of planetesimals throughout the disk with a particular set of planetary orbital parameters. We adopt the observational

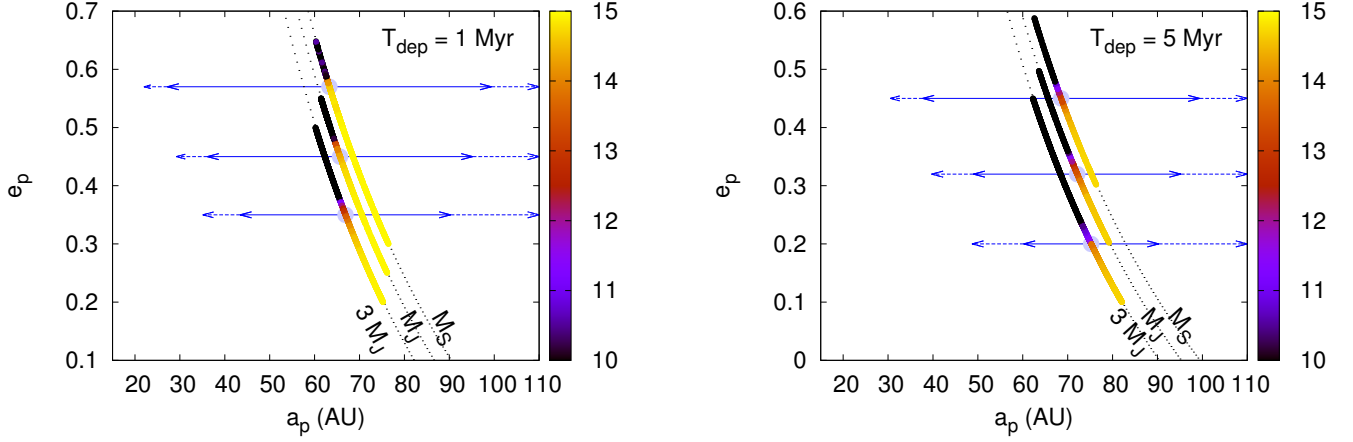


Figure 3. The location of planetesimals after the passage of a hypothetical planet’s sweeping secular resonance, as a function of its orbital parameters. In order to test impact of the sweeping secular resonance on Vega’s debris disk (Su et al. 2013), a set of test planetesimals are initially placed at its inner boundary, i.e. 15 AU. Their locations at $t = 10T_{\text{dep}}$ are represented by colors with the scale indicated in the reference bar on the right hand side of the left (for $T_{\text{dep}} = 1$ Myr) and right (for $T_{\text{dep}} = 5$ Myr) panels. The light blue dots label the critical values of a_p and e_p which demarcate the planet’s kinematic properties which may lead to significant orbital evolution for the perturbed planetesimals. The solid blue line (with arrows) indicate the extent of an eccentric planet’s radial excursion. The dashed blue arrows refer its chaotic zone as calculated using Equation (3).

upper limit ($3M_J$) for M_p . Based on the results in Figure 3, we adopt $a_p = 75$ AU, $e_p = 0.2$, and $T_{\text{dep}} = 5$ Myr. We place a population of 9×10^3 representative planetesimals with a uniform semi-major axis and azimuthal distribution between 5 – 150 AU from the host star. These planetesimals all have zero initial eccentricity. Although the planet’s inner and outer secular resonance sweep past a_{int} and a_{ext} within $t = 3T_{\text{dep}}$ (Fig. 2), we compute the planetesimals’ orbital evolution to $t = 10T_{\text{dep}}$ and plot, in Figure 4, their retention fraction in equally-spaced (5 AU) bins of semi-major axis. This retention fraction is statistically computed from the ratio of final to initial number of planetesimals in each bin.

In order to distinguish between the effects of dynamical instability and sweeping secular resonances, we carry out additional series of simulations of a purely N -body system. Without the contribution to the potential from any residual gas, the hypothetical planet does not precess

and induce secular resonances to the planetesimals. Nevertheless, it induces both main motion and eccentric resonances to destabilize the orbits of nearby planetesimals.

In the absence of a gas potential, the survival fraction of planetesimals is mainly dominated by two competing gravitational interactions, that of the host star and that of the giant planet, respectively. In Figure 4, the bottom panel shows that under the perturbation of gas giant, most planetesimals ($> 95\%$) within the planet’s chaotic zone (red arrows label region separated from perihelion and apohelion) are scattered from their original locations. Most planetesimals can survive within 50 AU or external to 110 AU (two exceptions around 98 AU and 105 AU), roughly beyond the chaotic zone. It explains the observed features of cold belt’s truncated region, but fails to fit the outer boundary of the warm belt in infrared observation (~ 15 AU) under the lone-planet’s scattering. However, taking a depleting gas disk into

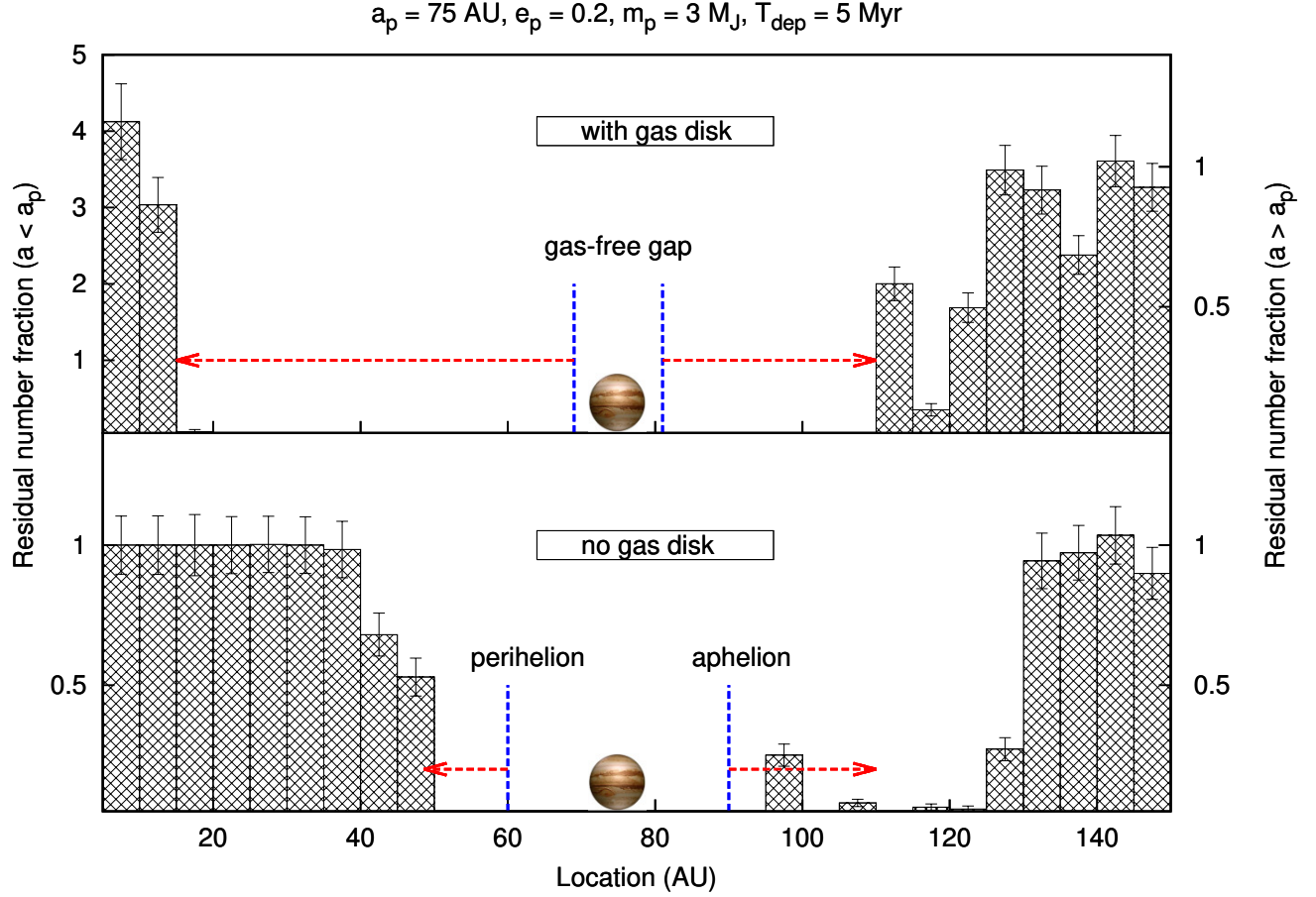


Figure 4. Residual number fraction as a function of planetesimals’ location. The top panel shows the model with gas disk, and includes the gravitational potential and gas drag effect, while the bottom panel shows the results of pure N -body interactions without a gas disk. The planet symbol indicates the semi-major axis of the giant planet (not to scale). In the top panel, the blue lines map out the gas-free zone around the planet, and red arrows map out the region where planetesimals are expected to be completely cleared (dust-free gap boundary indicate by observation). In the bottom panel, blue lines in the no-gas model, label the perihelion and aphelion of the planet, and red arrows point to the boundary of the chaotic zone.

consideration, a large amount of planetesimals (especially for those within the orbit of giant planet) are excited along the sweeping path of secular resonance and subsequently orbital decay by gas drag, thus an extended planetesimal-free region is cleaned out, shown in the top panel of Figure 4.

As most of planetesimals within 45 AU (inner boundary of chaotic zone) are swept inward and assemble within 15 AU, this result is consistent with the observed boundaries of warm belt in Vega system. Also, within 15 AU, the number

of planetesimals has roughly quadrupled by the end of the simulation. The latter suggests frequent collisions in this region, and perhaps that even the formation of super-Earths may be possible in the warm belt. Thommes et al. (2008) studied the formation of the terrestrial planets in our Solar system resulting from the sweeping secular resonances of the giant planets, and suggests that a planet may form or is in the process of forming in the warm debris disk of Vega.

In the simulations with a circumstellar gas disk, the location of the outer mass collection

is consistent with the observed infrared boundaries of the cold belt in Vega system (Su et al. 2013). This indicates that even though the secular resonance sweeps through the gas disk in both directions (both inwards and outwards), the clearing effect caused by the sweeping secular resonance mechanism in the cold belt region is ineffective. It can be ignored because the inward migrations of planetesimals caused by damping is in the opposite direction to the secular resonance sweeping. Besides, the surface density of gas disk at large distances declines rapidly, making it hard to damp planetesimals and hence their orbital decay can be ignored. Therefore, applying the outer chaotic zone as one of boundary constraints to confine the orbital parameter of an unseen planet is reasonable and valid in the lone-planet scenario.

Interestingly, in pure N -body simulations, the mass assembly in the cold belt region is not completely truncated at 110 AU which is estimated to be chaotic boundary, there is still a non-negligible number of planetesimals isolated gathering at several semi-major axes between roughly 95 AU and 110 AU. To understand this anomaly in the mass assembly, we further discuss the distribution of planetesimals' orbital parameters after 50 Myr of evolution. In Figure 5, detailed accounting for residual planetesimals shows that even though a planet can scatter most planetesimals from its chaotic zone, in the gas-free environment, there are still some 'lucky' planetesimals that can survive as they are captured into a powerful mean motion resonance, for example the 3:2 and 5:3 resonances, of the giant planet. Outside the chaotic zone, the eccentricities of planetesimals oscillate with large uncertainty due to the giant planet's secular perturbation. While in a depleting gas disk, planetesimals which are swept through and captured by the secular resonance of giant planet are mostly excited to some certain eccentricity and can maintain this value due to weak damp-

ing. It provides us a clue to make a rough judgement about whether the configuration of the two-belt debris disk is the result of sweeping secular resonance before the gas is completely depleted by measuring the eccentricity dispersion of the bodies in the cold belt.

In Figure 6, we illustrate the possible configurations which may account for the entire $\sim 15 - 110$ AU dust free gap in the Vega system. Considering the depletion timescale of the gas disk in the Vega system likely varies from ~ 1 Myr to ~ 5 Myr (with a large uncertainty), the possible planet candidates are also expected to be detected in wide range of regions, especially for a low mass planet, e.g., a Saturn-mass planet which can generate observable features in our scenario can be between ~ 25 AU and ~ 100 AU from the host star. Even for a $3M_J$ mass planet (upper limit), its detectable distance is $\sim 45 - 90$ AU.

3. APPLICATION TO THE FOMALHAUT SYSTEM

The Fomalhaut system is often treated as a sibling of the Vega system, since both systems have a host star of spectral type A, similar masses and ages, and both host a similar debris disk (Su et al. 2013). According to Su et al. (2013), the dust-free gap in the debris disk of Fomalhaut extends from ~ 10 AU to ~ 140 AU, which is slightly larger than the gap of the Vega system. It is therefore worthwhile considering a similar formation scenario for the dust-free gap in the Fomalhaut system.

Similar to the method applied to the Vega system, we primarily set some test planetesimals located at 10 AU to constrain the inner boundary. The outer boundary is based on the calculation using Equation 3, assuming the apocenter of the gas giant is one chaotic zone width from the cold belt. And as inferred by Kenworthy et al. (2009), the ground-based high-contrast observations provide us a $2M_J$ upper mass limit for any planet located between 10 – 40 AU. There-

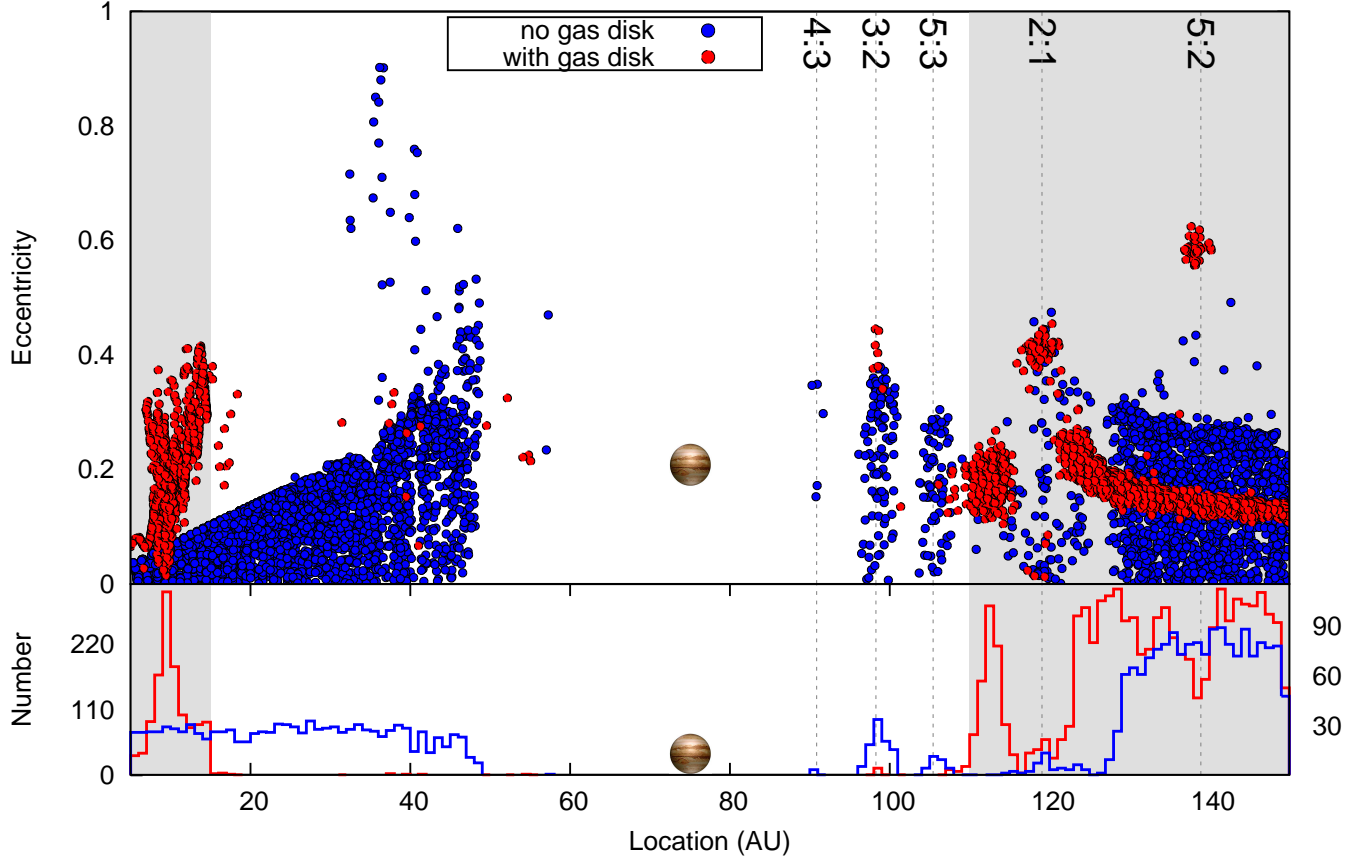


Figure 5. The distribution of test planetesimals at time 50 Myr. A three Jupiter mass planet is located at 75 AU with eccentricity equal to $e = 0.2$. The red and blue colors label the case that planetesimals evolve in a depleting gas disk and without a gas disk, respectively. The top panel shows the eccentricity distribution of planetesimals as a function of their locations, while the bottom panel statistically counts the planetesimals’ number distribution in detail (planetesimals whose semi-major axis inside and outside of the giant planet are plotted separately, as indicated by the left and right axes). The planet symbol indicates the semi-major axis of the giant planet (not to scale). Several mean motion resonance locations in the cold belt region are indicated with the dashed vertical lines, and the warm and cold debris belt regions are marked by the grey-shaded areas.

fore, we mainly explore the possibility of a hypothetical lone-planet with a mass $M_p = M_S$, M_J , $2M_J$. We vary the planet’s orbital eccentricity e_p , semi-major axis a_p , and disk depletion time scale T_{dep} in an attempt to reproduce the observed two-belt structure in Figure 7. In comparison with the Vega system, our successful models require a large eccentricity and a relatively large ($\sim 70 - 80$ AU) semi-major axis to

open the wide dust-free gap in the Fomalhaut system.

For example, a $M_p = 2M_J$ planet can induce the observed gap with $a_p \sim 76$ AU and $e_p \sim 0.5$ in a disk with $T_{\text{dep}} = 5$ Myr. The results of other successful models are shown in Figures 8 and 9. These boundary conditions can lead to the severe clearing of planetesimals from the observed gap region and their migration to a region ~ 10 AU. The population of resid-

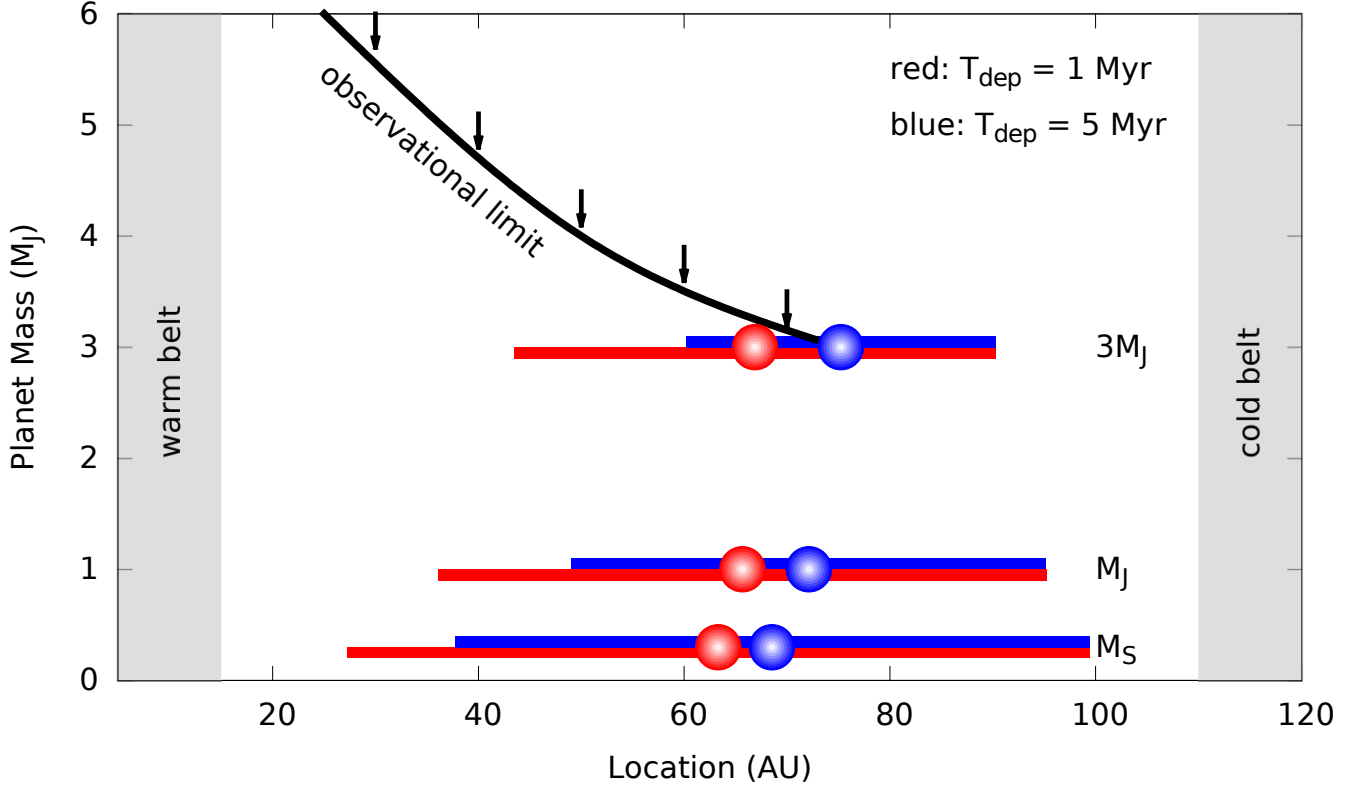


Figure 6. A schematic view of the potential planetary architectures of the Vega system that can account for the large dust-free gap between warm and cold debris belts (grey shadowed regions). The red and blue dots present the possible semi-major axis and mass of an (unseen) planet according to the boundary constraints, while colored bars indicate the possible range of distances of each planet from the host star. Colors represent different evolving timescales of the gas disk, $T_{\text{dep}} = 1$ Myr (red) and $T_{\text{dep}} = 5$ Myr (blue). The observational limit from direct imaging for planets around Vega result from [Marois et al. \(2006\)](#) and [Heinze et al. \(2008\)](#) is also indicated.

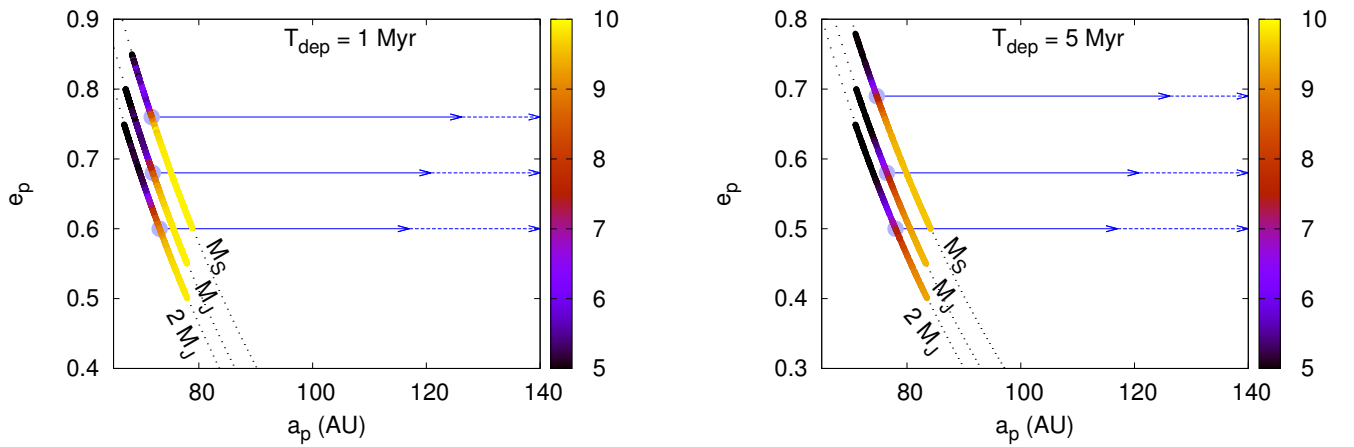


Figure 7. As in Figure 3, a depleting gas disk with two dissipation timescales, 1 Myr and 5 Myr, are discussed separately.

ual planetesimals in the inner ring increases by ~ 5.5 times its original value. All planetesimals within the planet’s aphelion are cleared through orbit crossing and close encounters. Beyond 140 AU, residual planetesimals are essentially unperturbed and form an outer ring. Near the inner boundary of the outer ring, some residual planetesimals accumulate near the planet’s mean motion resonances, especially its 2:1 mean motion resonance. These local concentrations are separated from the continuous mass distribution of the outer cold belt, and they may contribute to the subsequent formation of additional dwarf planets.

Our assumptions in the lone-planet scenario are not in conflict with what is known about the Fomalhaut system. According to the optical observations of Kalas et al. (2008), an exoplanet candidate was first presented in Fomalhaut system, named as Fomalhaut b. This planet may have dynamically sculpted the ring-like outer debris disk around Fomalhaut (Chiang et al. 2009). Even though the existence of this planet remains controversial (Lawler et al. 2015), its observationally inferred separation by Kalas et al. (2008) (~ 115 AU) is consistent with the estimated apastron of our hypothetical lone planet with $a_p = 76$ AU and $e_p = 0.5$ (see Figure 10). We note that the orbital data for Fomalhaut b in *NASA Exoplanet Archive* suggest that the eccentricity of this candidate should be larger than 0.13 and its mass is 2.6 ± 0.9 times of the mass of Jupiter mass. Therefore, if the existence of Fomalhaut b is indeed confirmed, it may be a good culprit for inducing the large dust-free gap in the debris disks of the Fomalhaut system.

4. SUMMARY AND DISCUSSIONS

Infrared observations have indicated large dust-free gaps in the debris disks of both Vega and Fomalhaut. Up to now, the origin of these wide gaps have been attributed to the dynamical perturbation of (yet to be detected) multiple gas giants. However, actual observational

data do not support this theoretical hypothesis. With the exception of the HR8799 system, no Vega-like systems have been found to host multiple planets. In this paper, we put forward the lone-planet model. We show that due to the sweeping secular resonance effect, one planet with a modest eccentricity and mass (a few M_J) is adequate to open very wide gap in the debris disk during the epoch of gas depletion.

We apply the lone-planet hypothesis to the Vega system. In this case, a $M_p = 3M_J$ with a relatively small $e_p \sim 0.2$ and $a \sim 75$ AU would be sufficient to open and maintain a wide gap which resembles the observed debris distribution. We constructed a similar model for the Fomalhaut system. For the wider gap in this system, a $M_p = 2M_J$ planet with an eccentricity $e_p \sim 0.5$ and semi-major axis $a_p \sim 76$ AU, would successfully clear most of residual planetesimals from 10 AU to 140 AU during the disk depletion. From these results, we infer that (1) the inner boundary of the cold belt is mainly cleared by the gas giant’s gravity, from the cold belt near one chaotic zone width; (2) the outer boundary of the warm belt is dominated by secular resonance’s sweeping path.

Finally, our results indicate that the powerful cleaning effect of the sweeping secular resonance along its path, does not only impact on the kinematic configuration in our own Solar system but also influences other exoplanet systems. All planetary systems are born in a circumstellar disk. A significant fraction ($\sim 15 - 20\%$) of solar type stars and larger fraction of more massive stars contain one or more gas giants. Up on the emergence of these massive planets, the sweeping secular resonance would occur naturally during the depletion of the disk provided they have at least a modest eccentricity. As it propagates throughout the disk, eccentricity of a population of residual planetesimals is excited. The depleting disk gas also damp their eccentricity and induce their orbital decay. The

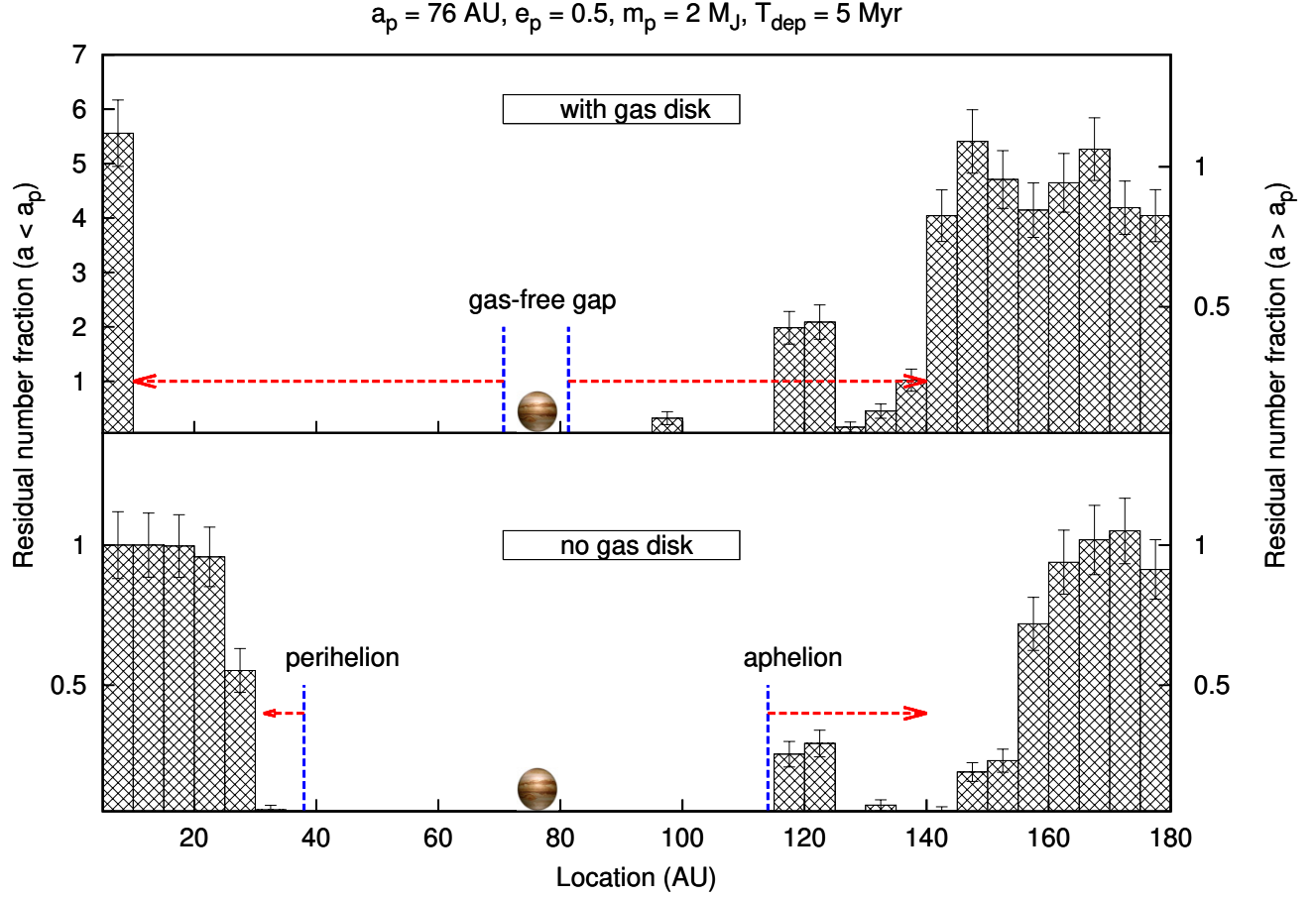


Figure 8. As in Figure 4, but with a planet mass of two-Jupiter masses, which has a semi-major axis of 76 AU and an eccentricity of 0.5.

combined influence of the sweeping secular resonance and gas damping of planetesimals can produce a large dust-free gap. In the current work, we used this lone-planet hypothesis to infer the origin of wide gaps in Vega and Fomalhaut systems, and it is also possible to extend this scenario to other double-ring debris disks in the future.

ACKNOWLEDGMENTS

This work was supported by the National Science Foundation of China (Grant No. 11333003, 11390372). M.B.N.K. was supported by the National Natural Science Foundation of China (grants 11010237, 11050110414, 11173004, and 11573004) and the Research Development Fund (grant RDF-16-01-16) of Xi'an Jiaotong-Liverpool University (XJTLU).

Software: HERMIT4 (Aarseth 2003)

REFERENCES

- | | |
|---|--|
| <p>Aarseth S. J. 2003, Gravitational N-Body Simulations. Cambridge Univ. Press, Cambridge (ISBN 0521432723)</p> | <p>Adachi, I., Hayashi, C., & Nakazawa, K. 1976, Prog. Theor. Phys., 56, 1756</p> <p>Agnor, C. B., & Lin, D. N. C. 2012, ApJ, 745, 143</p> <p>Artymowicz, P. 1993, ApJ, 419, 166</p> |
|---|--|

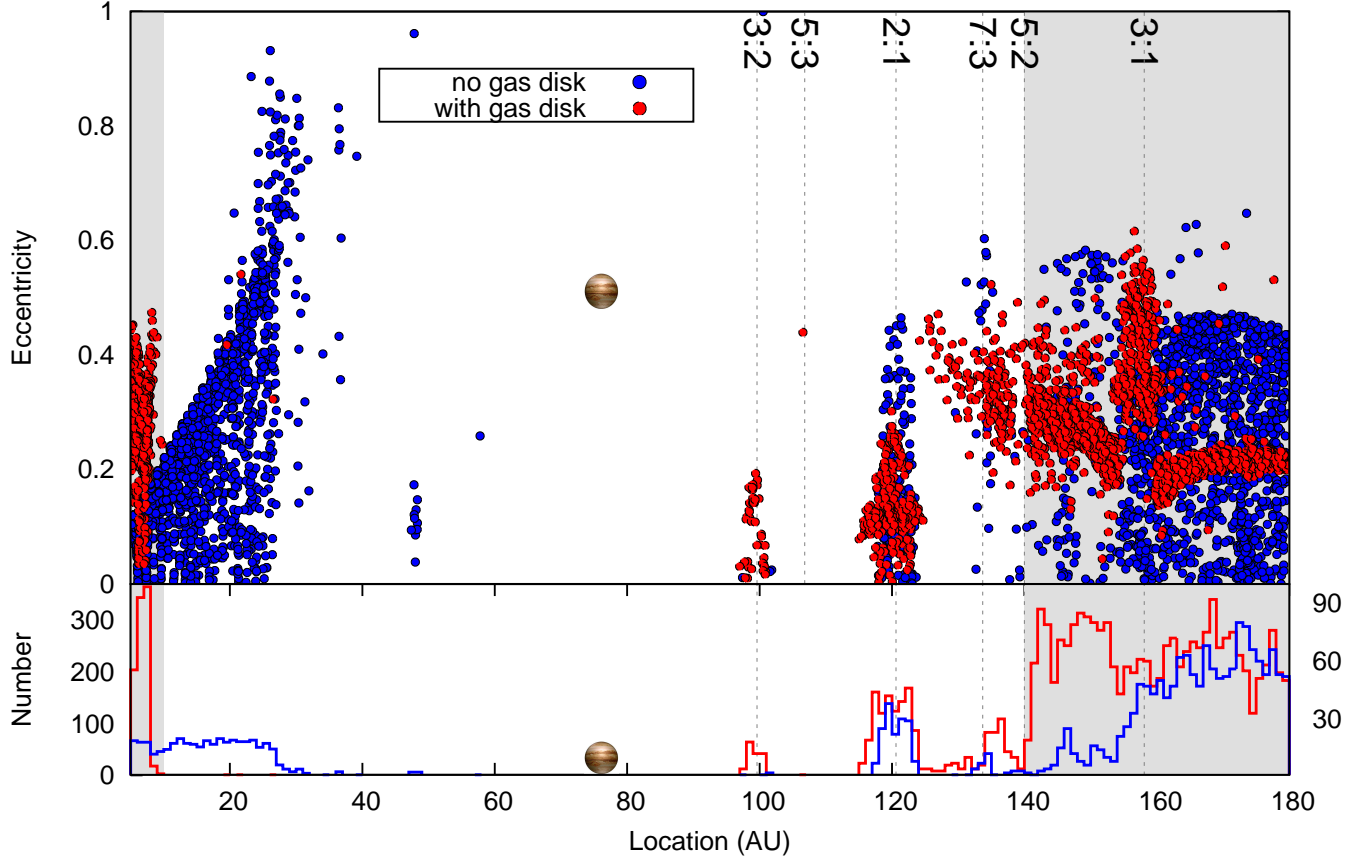


Figure 9. As in Figure 5, but with a planet mass of two-Jupiter mass, which has a semi-major axis of 76 AU and an eccentricity of 0.5.

Backman, D. E., & Paresce, F. 1993, in *Protostars and Planets III*, eds. E. H. Levy, & J. I. Lunine, 1253

Backman, D., Marengo, M., Stapelfeldt, K., et al. 2009, *ApJ*, 690, 1522

Boley, A. C., Payne, M. J., Corder, S., Dent, W. R. F., Ford, E. B., & Shabram, M. 2012, *ApJ*, 750, L21

Bonnefoy, M., Milli, J., et al. 2017, *A&A*, 597, L7

Brasser, R., Morbidelli, A., Gomes, R., Tsiganis, K., Levison, H. F. 2009, *A&A*, 507, 1053

Bromley, B. C., & Kenyon, S. J. 2017, *AJ*, 153, 216

Bryden, G., Rozyczka, M., Lin, D.N.C., Bodenheimer, P. 2000, *ApJ*, 540, 1091

Chiang, E., Kite, E., Kalas, P., Graham, J. R., & Clampin, M. 2009, *ApJ*, 693, 734

Clanton, C., & Gaudi, B. S. 2016, *ApJ*, 819, 125

Duncan, M., Quinn, T., & Tremaine, S. 1989, *Icarus*, 82, 402

Gomes, R. S., Levison, H. F., Tsiganis, K., & Morbidelli, A. 2005, *Nature*, 435, 466

Hayashi, C., Nakazawa, K., & Nakagawa, Y. 1985, in *Protostars and Planets II*, ed. by D. C. Black & M. S. Matthews (Tucson: Univ. Arizona Press), 1100

Heinze, A. N., Hinz, P. M., Kenworthy, M., Miller, D., & Sivanandam, S. 2008, *ApJ*, 688, 583

Heppenheimer, T. A. 1980, *Icarus*, 41, 76

Hosseini, A. P., Edgar, R. G., Quillen, A. C., & Lepage, A. 2007, *MNRAS*, 378, 966

Rameau, J., Chauvin, G., Lagrange, A. M., et al. 2013, *ApJ*, 779, L26

Rameau, J., Nielsen, E. L., et al. 2016, *ApJL*, 822, L29

Ida, S., & Lin, D. N. C. 1996, *AJ*, 112, 1239

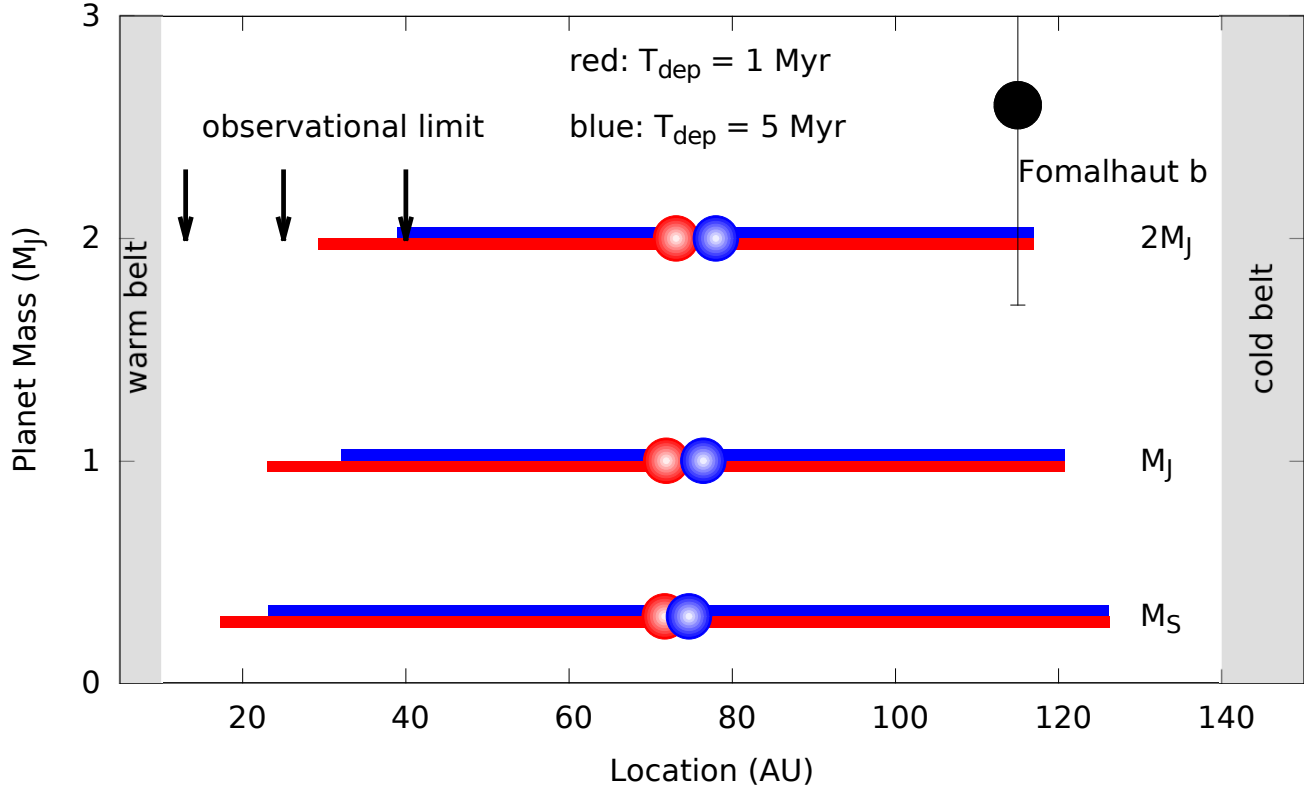


Figure 10. An overall view of the potential planetary architecture in the Fomalhaut system, as Figure 6. According to [Kenworthy et al. \(2009\)](#), any planet orbiting between $\sim 15 - 40$ AU with mass $> 2M_J$ is detectable.

Janson, M., Carson, J. C., Lafreniere, D., Spiegel, D. S., Bent, J. R., & Wong, P. 2012, *ApJ*, 747, 116

Kalas, P., Graham, J. R., Chiang, E., et al. 2008, *Science*, 322, 1345

Kenworthy, M. A., Mamajek, E. E., Hinz, P. M., et al. 2009, *ApJ*, 697, 1928

Lawler S. M., Greenstreet S., Gladman B., 2015, *ApJ*, 802, L20

Marois, C., Lafreniere, D., Doyon, R., Macintosh, B., & Nadeau, D. 2006, *ApJ*, 641, 556

Marois, C., Macintosh, B., Barman, T., et al. 2008, *Science*, 322, 1348

Marois, C., Zuckerman, B., Konopacky, Q. M., Macintosh, B., & Barman, T. 2010, *Nature*, 468, 1080

Morales F. Y., Bryden G., Werner M. W., Stapelfeldt K. R. 2013, *ApJ*, 776, 111

Morrison, S., & Malhotra, R. 2015, *ApJ*, 799, 41

Murray, C. D., Dermott, D. F. 1999, *Solar system Dynamics*. Cambridge Univ. Press, Cambridge

Mustill, A. J., & Wyatt, M. C. 2012, *MNRAS*, 419, 3074

Nagasawa, M., Lin, D. N. C., & Ida, S. 2003, *ApJ*, 586, 1374

Nagasawa M., Lin D., Thommes E. 2005, *ApJ*, 635, 578

Levison, H. F., Morbidelli, A., VanLaerhoven, C., & Gomes, R. 2008, *Icarus*, 196, 258

Lin, D. N. C., & Papaloizou, J. 1986, *ApJ*, 309, 846

Su, K. Y. L., et al. 2005, *ApJ*, 628, 487

Su, K. Y. L., Rieke, G. H., Stapelfeldt, K. R., et al. 2009, *ApJ*, 705, 314

Su, K. Y. L., Rieke, G. H., Malhotra, R., et al. 2013, *ApJ*, 763, 118

Su, K. Y. L., Morrison, S., Malhotra, R., et al. 2015, *ApJ*, 799, 146

Su K. Y. L. et al., 2017, *AJ*, 153, 226

Supulver K. D., Lin D. N. C. 2000. *Icarus* 146, 525

Thommes, E., Nagasawa, M., & Lin, D. N. C. 2008, *ApJ*, 676, 728

Ward, W. R. 1981, *Icarus*, 47, 234

- Ward, W. R. 1989, *ApJ*, 345, L99
Ward, W. R. 1993, *Icarus*, 106, 274
Weidenschilling, S. J. 1977, *MNRAS*, 180, 57
Wisdom, J. 1980, *AJ*, 85, 1122
Wyatt, M. C., & Dent, W. R. F. 2012, *MNRAS*, 424, 1206
Yoon J., Peterson D. M., Kurucz R. L., Zagarelio R. J., 2010, *ApJ*, 708, 71
Zheng, X. C., Lin, D. N. C., & Kouwenhoven, M. B. N. 2017, *ApJ*, 836, 207
Zhou, J. L., Lin, D. N. C., & Sun, Y. S. 2007, *ApJ*, 666, 423
Zhu, Z., Nelson, R. P., Hartmann, L., Espaillat, C., & Calvet, N. 2011, *ApJ*, 729, 47
Zhu, Z., Nelson, R. P., Dong, R., Espaillat, C., & Hartmann, L. 2012, *ApJ*, 755, 6